Oxygen-Transfer Reactions of Methylrhenium Oxides

Mahdi M. Abu-Omar,[†] Evan H. Appelman,[‡] and James H. Espenson*,[†]

Department of Chemistry, Iowa State University, Ames, Iowa 50011, and Chemistry Division,
Argonne National Laboratory, Argonne, Illinois 60439

Received June 14, 1996[⊗]

Methylrhenium dioxide, CH_3ReO_2 (or MDO), is produced from methylrhenium trioxide, CH_3ReO_3 (or MTO), and hypophosphorous acid in acidic aqueous medium. Its mechanism is discussed in light of MTO's coordination ability and the inverse kinetic isotope effect (kie): $H_2P(O)OH$, $k = 0.028$ L mol^{-1} s^{-1}; $D_2P(O)OH$, $k = 0.039$ L mol^{-1} s^{-1}. The Re(V) complex, MDO, reduces perchlorate and other inorganic oxoanions (XO_n^-, where X = Cl, Br, or I and $n = 4$ or 3). The rate is controlled by the first oxygen abstraction from perchlorate to give chlorate, with a second-order rate constant at pH 0 and 25 °C of 7.3 L mol^{-1} s^{-1}. Organic oxygen-donors such as sulfoxides and pyridine *N*-oxides oxidize MDO to MTO as do metal oxo complexes: $VO^{2+}{}_{(aq)}$, $VO_2{}^+{}_{(aq)}$, $HOMoO_2{}^+{}_{(aq)}$, and MnO_4^-. The reaction between $V^{2+}{}_{(aq)}$ with MTO and the reduction of VO^{2+} with MDO made it possible to determine the free energy for MDO/MTO. Oxygen-atom transfer from oxygen-donors to MDO involves nucleophilic attack of X−O on the electrophilic Re(V) center of MDO; the reaction proceeds via an [MDO·XO] adduct, which is supported by the saturation kinetics observed for some. The parameters that control and facilitate the kinetics of such oxygen-transfer processes are suggested and include the force constant for the asymmetric stretching of the element−oxygen bond.

Introduction

Our subject is the kinetics and thermodynamics of transfer of an oxygen atom from a donor to an acceptor and the correlation of the data for the kinetics of a family of such reactions in terms of their mechanism. The mobility of oxygen atoms among rhenium compounds in particular has been reviewed, and thermodynamic data for many such reactions has been described.[1] These issues arose in research into certain catalytic reactions of methylrhenium trioxide (CH_3ReO_3, abbreviated as MTO), where it became apparent that a reduced species $CH_3ReO_2L_n$ (L = here a solvent or, in general, a ligand) was formed.[2,3] In aprotic solvents (toluene, benzene, chloroform) triphenylphosphine proved to be a suitable acceptor. In water hypophosphorous acid serves quite well. With the unknown degree of hydration of CH_3ReO_2 aside for now, the equation for its formation is

$$CH_3ReO_3 + H_2P(O)OH \rightarrow CH_3ReO_2 + HP(O)(OH)_2 \quad (1)$$

Methylrhenium dioxide (MDO) is a strong 2e reducing agent able to abstract an oxygen atom from many substrates. Suitable partners are oxoanions (XO_n^-, including even the notoriously nonreactive ClO_4^-, as presented in a previous communication),[4] organic oxides (amine oxides, sulfoxides, epoxides, etc.), and certain oxo−metal species such as VO^{2+}. Our goal has been to provide data for these reactions and their kinetics and thermodynamics. We have also defined structural and electronic factors that control the reactivity. To no surprise, the reaction rates could not be successfully correlated in a Marcus sense with the overall driving force, presumably because the overall driving force so poorly represents the species that emerge from the transition state. Also, the intrinsic O-transfer rates (self-exchange) are in general not known. On the other hand, we have been able to some extent to relate the rate constant values to the element−oxygen force constants.

MDO is without doubt oxidized, but the term electron transfer will be avoided. It is used in the literature both to designate redox processes in general and to specify a particular mechanism. There is also no call at this stage to identify a perhaps problematic (but perhaps valid) relation between our subject and certain other oxidation−reduction reactions that proceed by an inner-sphere mechanism said to involve atom transfer. The large majority of those cases lead also to a single unit of oxidation state change, which is not so here. In a quite different chemical context this distinction has been addressed very thoughtfully in the literature.[5]

Since oxygen-transfer processes are important industrially and biologically, many catalytically-active transition metal complexes have been studied, including molybdenum(V) and -(VI),[6,7] ruthenium(V) and -(IV),[8,9] rhenium(V),[10,11] and ruthenium(II).[12,13] The literature also includes examples of the transfer of oxo ligands in oxometalloporphyrin systems: $Mo^{VI}(TPP)(O)_2$,[14] $Fe^{IV}(TPP)(O)$,[15] and $Ru^{VI}(TMP)(O)_2$[16] [TPP = 5,10,15,20-tetraphenylporphyrinato; and TMP = 5,10,15,20-tetramesitylporphyrinato]. In recent developments, the photo-

---

[†] Iowa State University.

[‡] Argonne National Laboratory.

[⊗] Abstract published in *Advance ACS Abstracts,* December 1, 1996.

(1) Holm, R. H.; Donahue, J. P. *Polyhedron* **1993**, *12*, 571.

(2) Herrmann, W. A.; Roesky, P. W.; Wang, M.; Scherer, W. *Organometallics* **1994**, *13*, 4531.

(3) Zhu, Z.; Espenson, J. H. *J. Mol. Catal.* **1995**, *103*, 87.

(4) Abu-Omar, M. M.; Espenson, J. H. *Inorg. Chem.* **1995**, *34*, 6239.

(5) Schwarz, C. L.; Bullock, R. M.; Creutz, C. *J. Am. Chem. Soc.* **1991**, *113*, 1225.

(6) Caradonna, J. P.; Reddy, P. R.; Holm, R. H. *J. Am. Chem. Soc.* **1988**, *110*, 2139.

(7) Schultz, B. E.; Gheller, S. F.; Muetterties, M. C.; Scott, M. J.; Holm, R. H. *J. Am. Chem. Soc.* **1993**, *115*, 2714.

(8) Moyer, B. A.; Sipe, B. K.; Meyer, T. J. *Inorg. Chem.* **1981**, *20*, 1475.

(9) Kahn, M. T.; Rao, A. P.; Samad, S. A.; Chatterjee, D.; Bhatt, S. D.; Merchant, R. R. *Proc.-Indian Acad. Sci., Chem. Sci.* **1990**, *102*, 231.

(10) DuMez, D. D.; Mayer, J. M. *Inorg. Chem.* **1995**, *34*, 6396.

(11) Rybak, W. K.; Zagicek, A. *J. Coord. Chem.* **1992**, *26*, 79.

(12) Durham, B.; Wilso, S. R.; Hodgson, D. J.; Meyer, T. J. *J. Am. Chem. Soc.* **1980**, *102*, 600.

(13) Moyer, B. A.; Meyer, T. J. *J. Am. Chem. Soc.* **1979**, *101*, 1326.

(14) Ledon, H.; Bonnet, M. *J. Mol. Catal.* **1980**, *7*, 309.

(15) Chin, D. H.; La Mar, G. N.; Balch, A. L. *J. Am. Chem. Soc.* **1980**, *102*, 5945.

(16) Groves, J. T.; Quinn, R. *Inorg. Chem.* **1984**, *23*, 3844.

S0020-1669(96)00701-X CCC: $12.00

catalytic oxidation of hydrocarbons by a Mn(III) porphyrin complex utilizes ClO_4^- and IO_4^- as oxidants,[17] and bromide ions are oxidized by ClO_3^-, when catalyzed by a Mo(V) oxo complex.[18]

Oxides and oxo complexes of high-valent transition metals have attracted attention.[19−25] MTO in particular has a notable ability to catalyze reactions of hydrogen peroxide,[26−33] which it activates by coordination to the high-valent rhenium.[31,34,35] More recently, the ability of MTO to catalytically transfer “nitrene” and “carbene” moieties has been realized.[36] Reactions involving oxygen-atom transfer between rhenium (MDO and MTO) and a substrate (XO and X) can be explored in considerable detail, since the species involved are stable in aqueous, semiaqueous, and organic media.

Experimental Section

Materials. High-purity water was obtained by passing laboratory distilled water through a Millipore-Q water purification system. Perbromic acid was prepared from the fluorine oxidation of bromate.[37] Solutions of VO^{2+} in a triflate medium were obtained by adsorbing vanadyl ion from a solution of the vanadyl sulfate (Alfa) onto a column of Dowex 50W-X8 cation exchange resin, rinsing it free of sulfate ions, and eluting with 1.0 M HOTf. Solutions of V^{2+} were prepared by reduction of VO^{2+} with amalgamated zinc. $HOMo(O)_2(H_2O)_3^+$ was prepared by dissolving Na_2MoO_4 (J. T. Baker) in a HOTf medium.[38] Triphenylstibine oxide was prepared from the oxidation of triphenylstibine by H_2O_2 catalyzed by MTO.[29] $VO_2^+{}_{(aq)}$ was prepared by dissolving V_2O_5 (J. T. Baker) in aqueous HOTf. Most other chemicals were reagent grade and obtained commercially: MTO (Aldrich), hypophosphorous acid (J. T. Baker, 50% solutions in water), sodium hypophosphite (J. T. Baker), deuterated hypophosphorous acid (Aldrich, 50% solutions in D_2O), phosphorous acid (Aldrich), nitric acid (Fischer), sodium nitrite (Fischer), sodium chlorate (Fischer), perchloric acid (Fischer), sodium bromate (Fischer), sodium iodate (Fischer), potassium permanganate (Fischer), dimethyl sulfoxide (Fischer), phenyl methyl sulfoxide (Aldrich), *p*-tolyl methyl sulfoxide (Aldrich), phenyl vinyl sulfoxide (Aldrich), all pyridine *N*-oxides (Aldrich), and triphenylarsine oxide (Aldrich). Solutions of trifluoromethanesulfonic acid (triflic acid, HOTf) were obtained by carefully diluting the pure commercial material (Aldrich).

Reaction kinetics were studied in aqueous solutions for the most part; the aryl, alkyl sulfoxides and $Ph_3E{=}O$ (E = As, Sb) were studied in acetonitrile−water (1:1 or 3:1 v/v, as needed). All of these solutions contained 1.0 M HOTf to maintain a constant electrolyte medium and to stabilize MTO and MDO against polymerization in an aqueous medium.[22,23] The rate constants were determined at 25.0 ± 0.2 °C with Shimadzu UV-2101PC and UV-3101PC spectrophotometers and with an Applied Photophysics Sequential DS-17MV stopped-flow spectrometer. The buildup of MTO was followed at 270 nm ($\epsilon = 1300$ L mol^{-1} cm^{-1}).

The oxygen-donating agent was usually taken in large excess over MDO, and the reactions followed pseudo-first-order kinetics according to eq 2. When comparable concentrations of the two were taken, the data were fitted to eq 3 for mixed-second-order kinetics:

$$\mathrm{Abs_t} = \mathrm{Abs_\infty} + \{\mathrm{Abs_0} - \mathrm{Abs_\infty}\}e^{-k_\psi t} \qquad (2)$$

$$\mathrm{Abs_t} = \mathrm{Abs_\infty} + \frac{\{\mathrm{Abs_0} - \mathrm{Abs_\infty}\}\{m[\mathrm{B}]_0 - [\mathrm{A}]_0\}e^{-k_\psi t}}{m[\mathrm{B}]_0 - [\mathrm{A}]_0 e^{-k_\psi t}} \qquad (3)$$

where $[B]_0$ and $[A]_0$ are the initial concentrations, with $[B]_0$ the larger, and k_ψ represents $\{[B]_0 - [A]_0\}k$ in eq 2 and the nearly-equivalent quantity $\{[B]_0 - [A]_0/2\}k$ in eq 3; *k* is the bimolecular rate constant between a given oxygen-donor XO and MDO. The value of *m* in eq 3 is the stoichiometric consumption ratio of A to B in the overall equation, which is not necessarily unity should subsequent O-atom abstractions be much more rapid than the first.

Several reagents had large UV absorptions that masked that of MTO. Their rate constants were determined by competition experiments that used two substrates, one with a known rate constant. Product concentrations were determined from their integrated ^1H NMR signals during the initial stages (<10%) of the reaction. Equimolar amounts of the two competing reagents (∼0.1 M) were mixed with ∼0.1 M H_3PO_2 and ∼0.01 M MTO. After about one catalytic cycle (5−10% conversion, ∼20 min) the ^1H spectrum was recorded and integrated. As an example, one such substrate is PhS(O)Me. We paired it with Me_2SO. The ratio of the products in comparison with their starting concentrations allows the calculation of the missing value:

$$k_{\mathrm{PhS(O)Me}} = \frac{[\mathrm{PhSMe}]_t}{[\mathrm{Me_2S}]_t}(k_{\mathrm{Me_2SO}})\frac{[\mathrm{Me_2S}]_0}{[\mathrm{PhSMe}]_0} \qquad (4)$$

Product analysis was carried out with ^1H NMR for the organic substrates and MTO; the re-formation of MTO from the reaction of MDO and oxoanions was verified by the UV−vis and ^1H spectra of MTO. Chloride ions from the reduction of perchlorate were determined quantitatively by ion chromatography.[39] The formation of phosphorous acid in eq 1 was verified in aqueous and organic media by ^1H and ^{31}P NMR.

Results

Reaction of MTO and H_3PO_2. Repetitive scans for the progress of reaction 1 are shown in Figure 1, corresponding to the formation of MDO and H_3PO_3. Similar conditions were used for kinetics: 5.0×10^{-4} M MTO, 0.10−0.70 M H_3PO_2, and 1.0 M HOTf. The data were fitted to a biexponential equation to allow for intrusion of a slower second stage, discussed in the next section. The rate constant for reaction 1 is $(2.8 \pm 0.2) \times 10^{-2}$ L mol^{-1} s^{-1}. The high concentrations of hypophosphorous acid were needed to accelerate the reduction sufficiently to avoid the aforementioned oligomerization of MDO that occurs at longer times.

The kinetic isotope effect (kie) was investigated by using D_3PO_2 in D_2O. A similar analysis gave $k_D = (3.9 \pm 0.2) \times 10^{-2}$ L mol^{-1} s^{-1}. To confirm that the inverse kie arises from the P−H/P−D bond and not from the solvent or OH group, an experiment was conducted with H_3PO_2 in D_2O under conditions

---

(17) Suslick, K. S.; Acholla, F. V.; Cook, B. R. *J. Am. Chem. Soc.* **1987**, *109*, 2818.

(18) Villata, L. S.; Martire, D. O.; Capparelli, A. L. *J. Mol. Catal.* **1995**, *99*, 143.

(19) Herrmann, W. A.; Okuda, J. *J. Mol. Catal.* **1987**, *41*, 109.

(20) Herrmann, W. A. *Angew. Chem., Int. Ed. Engl.* **1988**, *27*, 1297.

(21) Herrmann, W. A. *J. Organomet. Chem.* **1990**, *382*, 1.

(22) Herrmann, W. A.; Fischer, R. W.; Scherer, W. *Adv. Mater.* **1992**, *4*, 653.

(23) Herrmann, W. A.; Fischer, R. W. *J. Am. Chem. Soc.* **1995**, *117*, 3223.

(24) Casey, C. P. *Science* **1993**, *259*, 1552.

(25) Edwards, P.; Wilkinson, G. *J. Chem. Soc., Dalton Trans.* **1984**, 2695.

(26) Espenson, J. H.; Pestovsky, O.; Huston, P.; Staudt, S. *J. Am. Chem. Soc.* **1994**, *116*, 2869.

(27) Vassell, K. A.; Espenson, J. H. *Inorg. Chem.* **1994**, *33*, 5491.

(28) Zhu, Z.; Espenson, J. H. *J. Org. Chem.* **1995**, *60*, 1326.

(29) Abu-Omar, M. M.; Espenson, J. H. *J. Am. Chem. Soc.* **1995**, *117*, 272.

(30) Al-Ajlouni, A. M.; Espenson, J. H. *J. Am. Chem. Soc.* **1995**, *117*, 9243.

(31) Herrmann, W. A.; Fischer, R. W.; Marz, D. W. *Angew. Chem., Int. Ed. Engl.* **1991**, *30*, 1638.

(32) Herrmann, W. A.; Fischer, R. W.; Schere, W.; Rauch, M. U. *Angew. Chem. Int. Ed. Engl.* **1993**, *32*, 1157.

(33) Kholopov, A. B.; Nikitin, A. V.; Rubailo, V. L. *Kinet. Catal.* **1995**, *36*, 101.

(34) Yamazaki, S.; Espenson, J. H.; Huston, P. *Inorg. Chem.* **1993**, *32*, 4683.

(35) Pestovsky, O.; van Eldik, R.; Huston, P.; Espenson, J. H. *J. Chem. Soc., Dalton Trans.* **1995**, 133.

(36) Zhu, Z.; Espenson, J. H. *J. Org. Chem.* **1995**, *60*, 7090.

(37) Appleman, E. H. *Inorg. Chem.* **1969**, *8*, 223.

(38) Cruywagen, J. J.; Heyns, J. B. B.; Rohwer, E. F. C. H. *J. Inorg. Nucl. Chem.* **1978**, *40*, 53.

(39) Barron, R. E.; Fritz, J. S. *J. Chromatogr.* **1984**, *316*, 201.

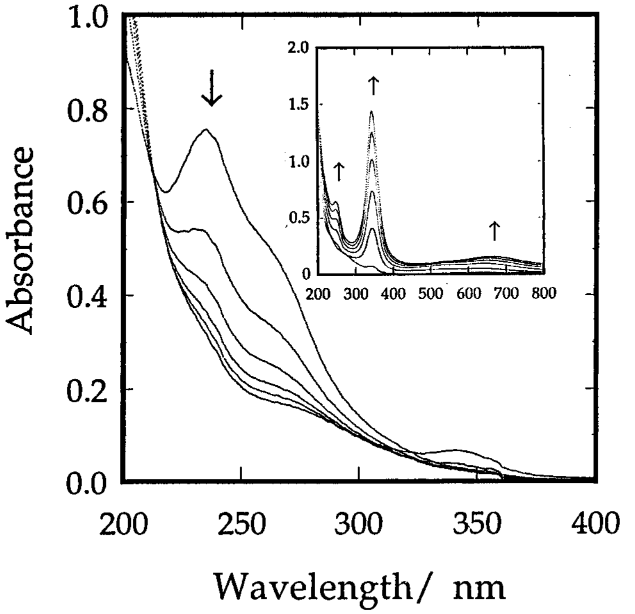

Figure 1. Spectral changes at 2 min intervals during the formation of MDO from MTO and H_3PO_2. Conditions: 0.2 mM MTO, 0.19 M H_3PO_2, 1.0 M HOTf, at 25 °C, optical path 2 cm. The inset shows at 12 min intervals the subsequent dimerization and oligomerization of MDO with 0.5 mM MTO, 0.70 M H_3PO_2.

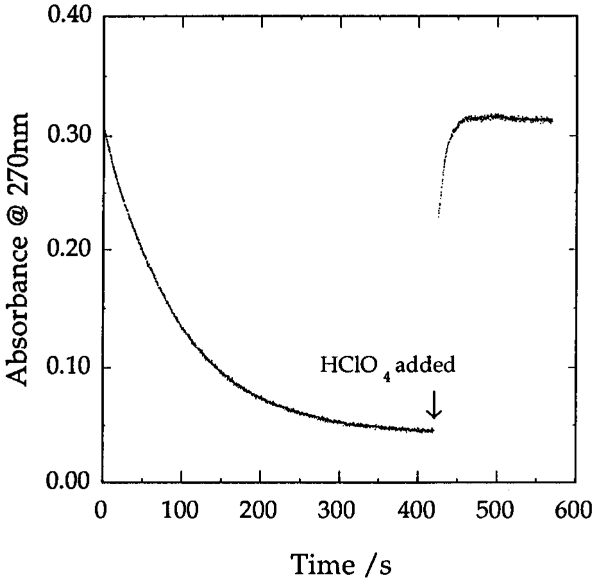

Figure 2. A time profile depicting initially the formation of MDO and then the regeneration of MTO. Conditions: 0.21 mM MTO, 0.40 M H_3PO_2, 1.0 M HOTf at 25.0 °C; at the arrow mark 4.0 mM $HClO_4$ was added.

where the MTO reaction occurs more rapidly than P−H exchange with the solvent.[40] The rate constant was the same as in H_2O.

The activation parameters were determined from the values of k over the range 5−48 °C. Least-squares fitting to the transition state theory expression (eq 5) resulted in these

$$k = \frac{k_B T}{h} e^{-\Delta H^{\ddagger}/RT} e^{\Delta S^{\ddagger}/R} \qquad (5)$$

values: $\Delta H^{\ddagger} = 12 \pm 1$ kcal mol^{-1}, $\Delta S^{\ddagger} = -27 \pm 2$ cal mol^{-1} K^{-1}.

Scheme 1

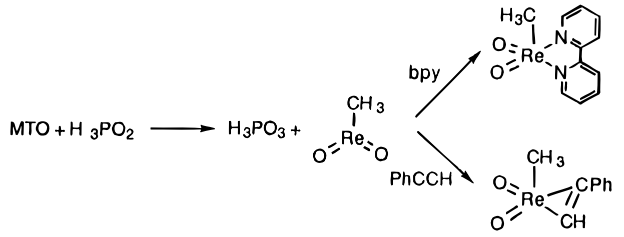

Oligomerization. At longer times during the reaction between MTO and excess H_3PO_2, a blue color was formed and then a blue-black precipitate was deposited. The spectral changes during that stage are shown in the inset to Figure 1. Its rate does not depend on the concentrations of H_3PO_3 or H_3PO_2, only on the total rhenium concentration. We therefore attribute the second stage to the dimerization and oligomerization of MDO, eq 6. Analogous oligomerization and polymerization reactions have been observed for MTO in more concentrated aqueous solutions.[22,23]

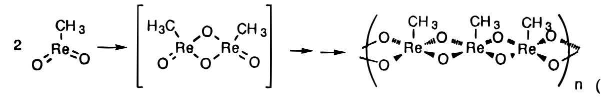
(6)

The sensitivity of the second stage to the total rhenium concentration is illustrated in Figure S-1 (Supporting Information: two absorbance−time recordings are displayed, one with rhenium taken at half the amount of the other). The concentration reduction greatly lowers the amount of $(MDO)_n$ formed. To avoid significant oligomer formation, $[Re]_T$ was kept in the range (1.0−2.5) × 10^{-4} M for the study of the kinetics.

MDO has also been prepared from MTO and PPh_3 in organic media, producing a species with coordinated phosphine or phosphine oxide.[2,41] In the present case we presume that one or more water molecules is coordinated to MDO, since $H_2PO_2^-$ and $H_2PO_3^-$ are so weakly coordinating and the solutions were maintained at pH 0 and their ^{31}P chemical shifts were unaltered. Further speciation of MTO has not been carried out, but other data can be cited. It has been established that MDO contains two oxo ligands. The absence of kinetic salt effects (over a narrow range, 0.2−1 M, however) was taken to show that MDO does not bear an ionic charge. The *sharply* pH dependent oligomerization of MDO limited the data to high [H^+] and high ionic strength.

To confirm that MDO is formed in eq 1, the reaction was run in acetonitrile and MDO trapped by 2,2′-bipyridine and by phenylacetylene, Scheme 1. The adducts were characterized by ^1H NMR and by IR, Table 1; the spectroscopic data agree with literature values.[41]

The Reduction of Anions by MDO. After the generation of ca. 2 × 10^{-4} M MDO from MTO (2 × 10^{-4} M) and 0.1−0.2 M H_3PO_2 and prior to $(MDO)_n$ formation, the desired oxoanion XO_n^- was added. The ensuing reaction, eq 7a,

$$XO_n^- + MDO \rightarrow XO_{n-1}^- + MTO \qquad (7a)$$

$$v = mk[MDO][XO_n^-] \qquad (7b)$$

restores the UV spectrum of MTO. Figure 3 depicts the initial formation of MDO and the quantitative restoration of MTO upon perchloric acid addition.

---

(40) Jenkins, W. A.; Yost, D. M. *J. Inorg. Nucl. Chem.* **1959**, *11*, 297.

(41) Felixberger, J. K.; Kuchler, J. G.; Herdtweck, E.; Paciello, R. A.; Herrmann, W. A. *Angew. Chem., Int. Ed. Engl.* **1988**, *27*, 946.

Table 1. ^{1}H NMR and IR Data for MDO Derivatives

Compound	^{1}H NMR ($CDCl_3$), δ/ppm	IR, ν/cm^{-1}
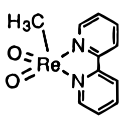	0.98 (s, Re-CH_3) 7.36 (t, *meta*-2H) 7.88 (t, *para*-2H) 8.37 (d, *meta*-2H) 8.75 (d, *ortho*-2H)	936 (s) 910 (vs)
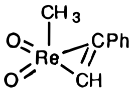	2.78 (s, Re-CH_3) 9.37 (s, *H*CCPh) 7.53 (m, HCC*Ph*) 7.82 (m, HCC*Ph*)	

The stoichiometric consumption of XO_n^- per MDO was investigated by spectrophotometric titrations and by the kinetics. The latter entails assuming a plausible value of m in eq 3 (for example, for the reaction between ClO_4^- and MDO, m might be 4 or 1). Only one of the values gave a proper fit of the data in a given case, and in that way the reaction stoichiometry could be determined. The reduction of the oxoanions by H_3PO_2 is entirely negligible on the time scale of their reduction by MDO, and much longer than that. The rate law for the oxoanions is given in eq 7b. Values of k and m are listed in Table 2.

The reduction of nitrate ions by MDO produces nitrous acid, characterized by its distinctive UV−vis spectrum. Since H_3PO_2 and NO_3^- were present at concentrations much higher than that of MTO, the rhenium complex is in effect a catalyst for oxygen transfer from NO_3^- to H_3PO_2. That is, reactions 1 and 7a occurring in sequence amount to Re-catalyzed O-atom transfer, not just for nitrate ions, but for all of the participating oxoanions.

In the particular case of NO_3^-, the situation changes after many cycles, as the accumulating nitrous acid, now more concentrated, begins to undergo decomposition, eq 8.[42]

$$3HONO \rightleftharpoons H^+ + NO_3^- + H_2O + 2NO \qquad (8)$$

Nitrous acid itself reacts with MDO. The rate constant was determined at a relatively low [HONO] = 5−20 mM to avoid its self-decomposition. MTO was formed as well as (we presume) hyponitrous acid, a *trans* dimer of “HON”,[43] the likely initial product, given the way this reaction follows the pattern observed for other oxoanions. Furthermore, since k(HONO) ≈ 10k(NO_3^-), the HONO formed from NO_3^- did not compete or interfere with the kinetics of the nitrate reduction stage since a >10× excess of NO_3^- was used.

The reaction with permanganate is much like the others, except faster. The first step may be taken to be, like the others, an oxygen-transfer reaction: $MnO_4^- + MDO \rightarrow \{MnO_3^-\} +$ MTO. Further reaction of the Mn(V) species is certain; no precipitate of MnO_2 was observed from these strongly acidic solutions, Mn^{2+} being the final product. This finding implicates H_3PO_2 as the source of the additional reducing equivalents for lower-valent manganese species.

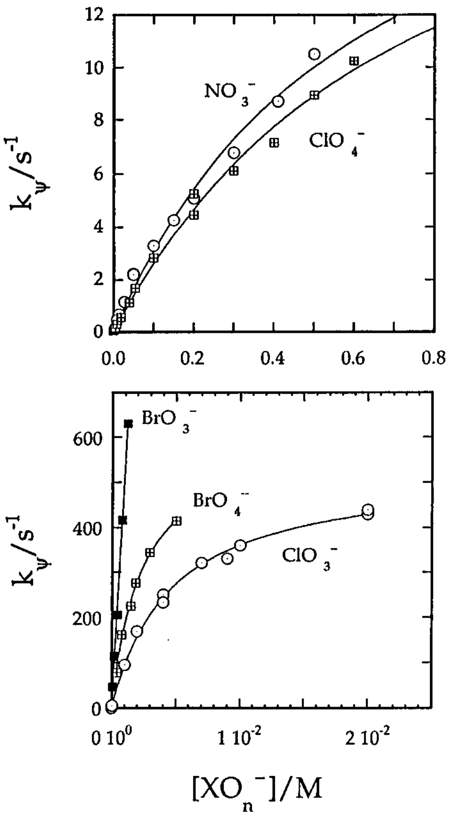

Figure 3. A group of plots of k_ψ versus $[XO_n^-]$ plots to illustrate the observed saturation kinetics in their reactions with MDO.

Table 2. Rate Constants for the Reaction of Methylrhenium Dioxide (MDO) with Oxoanions and Oxometal Complexes at pH = 0 and 25.0 °C

oxoanion	k_1/L mol^{-1} s^{-1}	stoichiometry MDO:XO_n^-
ClO_4^-	7.3 ± 0.2	4:1
ClO_3^-	(3.8 ± 0.2) × 10^4	3:1
BrO_4^-	(2.6 ± 0.2) × 10^5	1:1
BrO_3^-	(2.0 ± 0.2) × 10^5	3:1
IO_3^-	(1.2 ± 0.1) × 10^5	3:1
NO_3^-	(4.4 ± 0.2) × 10^1	1:1
MnO_4^-	1.0 × 10^6	3:2
HONO	(4.41 ± 0.30) × 10^2	1:1
VO_2^+	(9.9 ± 0.3) × 10^4	1:1
$HOMoO_2^+$	(6.0 ± 0.4) × 10^4	1:1

Rate Constant Plateaus. For many of the reactions, when higher $[XO_n^-]$ were used, the pseudo-first-order rate constants were no longer directly proportional to $[XO_n^-]$. As displayed in Figure 3, plots of k_ψ versus $[XO_n^-]$ attained a plateau at a high enough concentration of the anion. The curvature for perchlorate and nitrate ions occurs only at high concentration and might arise from a medium effect, in that neither anion is a perfect substitute for triflate ion in terms of activities even at constant ionic strength. The curvature for chlorate and perbromate ions, however, sets in at a low concentration of the anion and clearly cannot arise from a medium effect. Only for bromate ions did the plot of k_ψ versus $[BrO_3^-]$ remain linear throughout; here, however, the upper limit of rate constants by the stopped-flow technique limited the accessible concentration range. Thus, the curvature represents an authentic and general phenomenon, which can be interpreted in terms of a presumably oxygen-bridged intermediate:

$$MDO + XO_n^- \underset{k_{-1}}{\overset{k_1}{\rightleftharpoons}} [MDO{-}XO_n]^- \xrightarrow{k_2} MTO + XO_{n-1}^- \qquad (9)$$

---

(42) Bonner, F. T.; Donald, C. E.; Hughes, M. N. *J. Chem. Soc., Dalton Trans.* **1989**, 527.

(43) Akhtar, M. J.; Bonner, F. T.; Hughes, M. N. *Inorg. Chem.* **1985**, *24*, 1934.

The steady-state expression clearly does not apply, since it would not result in the reaction rate plateauing at high concentration. But a prior-equilibrium (pe) expression, eq 10 with $K = k_1/k_{-1}$, would do so, as would the even more general improved-steady-state expression (imp),[44] eq 11, which does not require the first step to be rapidly equilibrated prior to the second.

$$k_\psi^{\text{pe}} = \frac{Kk_2[\text{XO}_n^-]}{1 + K[\text{XO}_n^-]} \qquad (10)$$

$$k_\psi^{\text{imp}} = \frac{k_1k_2[\text{XO}_n^-]}{k_{-1} + k_2 + k_1[\text{XO}_n^-]} \qquad (11)$$

At the plateau both expressions lead to a limiting rate constant of k_2, because the rate saturates as adduct formation shifts toward the right. When two substrates were used together, in an effort to validate this proposal further, a situation was created in which a pair of such intermediates would be involved. The formation of both would jointly lower the reagent pool shared by each, giving rise to a significant and predictable rate retardation for the two together. The rates for mixed substrates are indeed slower than the sum of the rates of the independent reactions, supporting adduct formation. Efforts to make this a more quantitative treatment were frustrated, however, by all of the rates becoming so high that they pushed the reliable detection limit of the instrumentation.

Reactions with Oxo Metal Complexes. MTO and $V(H_2O)_6^{2+}$ react by O-atom transfer, and the process in fact is a reversible one, eq 12. The absorption of MTO centered at 270 nm fades initially and then rises in a second stage; concurrent with the latter is a new peak at 425 nm, attributed to $[V{-}O{-}V]^{4+}{}_{(aq)}$ of eq 13.[45]

$$CH_3ReO_3 + V^{2+}{}_{(aq)} \underset{k_{IV}}{\overset{k_{II}}{\rightleftharpoons}} CH_3ReO_2 + VO^{2+}{}_{(aq)} \qquad (12)$$

$$VO^{2+}{}_{(aq)} + V^{2+}{}_{(aq)} \xrightarrow{k} [V{-}O{-}V]^{4+}{}_{(aq)} + 2H^+ \overset{K}{\rightleftharpoons} 2V^{3+}{}_{(aq)} + H_2O \qquad (13)$$

The stopped-flow technique was used to study the kinetics under argon, since V^{2+} is air sensitive. The conditions were 0.15 mM MTO, 1.8−24 mM V^{2+}, pH 0 at 25.0 °C. The two stage reaction profiles were fitted to a biexponential function; the first-stage value of k_ψ was directly proportional to $[V^{2+}]$, giving $k_{II} = 68 \pm 1$ L mol^{-1} s^{-1}. The reverse reaction was studied by using H_3PO_2 to generate MDO; H_3PO_2 and VO^{2+} do not react. The rate constant so obtained is $k_{IV} = 193 \pm 5$ L mol^{-1} s^{-1}. Both rate constants were independent of $[H^+]$, although the range of variation was small owing to experimental limitations. The quotient affords the equilibrium constant $K_{12} = 0.35 \pm 0.01$. This value proved useful in defining the thermodynamics of the entire series of oxygen-transfer reactions.

Although $V^{3+}{}_{(aq)}$ is not oxidized by MTO, VO_2^+ transfers an oxygen to MDO. Stopped-flow kinetics were followed at $\lambda = 315$ nm with these concentrations: 0.25 mM MDO, 1.5−3.0 mM VO_2^+. The value of k_V (eq 14) is $(9.9 \pm 0.3) \times 10^5$

$$CH_3ReO_2 + VO_2^+{}_{(aq)} \xrightarrow{k_V} CH_3ReO_3 + [VO^+{}_{(aq)}] \xrightarrow{2H^+} V^{3+}{}_{(aq)} \qquad (14)$$

L mol^{-1} s^{-1}. The known reactions between V^{3+} and VO_2^+ and between H_3PO_2 and VO_2^+ were negligible on this time scale.

At pH <1, molybdenum(VI) is present primarily as the octahedral species $[HOMoO_2(OH_2)_3]^+$,[38] and molybdenum(V) as the dimer shown, having two bridging oxo groups and characterized by its distinctive absorption spectrum, $\lambda_{max} = 297$ ($\epsilon = 8 \times 10^3$ L mol^{-1} cm^{-1}) and 384 nm ($\epsilon = 1.6 \times 10^2$ L mol^{-1} cm^{-1}).[46]

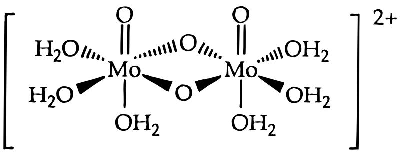

Mo(V) dimer

The reaction of MDO with Mo(VI) to produce MTO and the Mo(V) dimer was followed at 297 nm. One set of conditions was 0.10 mM MDO and 0.8−1.5 mM Mo(VI) and the other with excess MDO, 0.2−0.4 mM, and 0.02 mM Mo(VI), both with 1.0 M HOTf at 25.0 °C. Both sets of data fit first-order kinetics precisely. The second-order rate constants obtained from the quotient k_ψ/C_{xs} are $(6.4 \pm 0.3) \times 10^4$ and $(5.7 \pm 0.4) \times 10^4$ L mol^{-1} s^{-1} for the two excess reagents in the order listed. This result, obtained by a reversal of which reagent was taken in excess, constitutes a kinetic determination of the stoichiometry. Since the two average rate constants are the same within the experimental error, the reaction stoichiometry is given by the equation $2Mo^{VI} + 2MDO = 2MTO + [Mo^V]_2$.

We are inclined to discount direct formation of Mo(V) as the route to the dimer in this case, since in no other case was there any indication whatever of single electron transfer steps. More likely, this reaction, like the others, starts with O-atom transfer, forming oxomolybdenum(IV), previously recognized as a reactive transient.[46] Oxomolybdenum(IV) might then either react with molecular oxygen or disproportionate to yield the final Mo(V) dimer.[46,47] The involvement of molecular oxygen was ruled out by a direct test, this system being indifferent to its presence or exclusion, and the stoichiometry rules out disproportionation. The reaction of the Mo(IV) with H_3PO_2, present in substantial excess, seems the most likely explanation.

Organic Oxo Substrates. MDO was studied with sulfoxides, pyridine *N*-oxides, Ph_3AsO, and Ph_3SbO. The pyridine *N*-oxides and DMSO are sufficiently soluble to allow the use of water as the solvent. The others are not, however, and mixed acetonitrile−water media were used.

Since DMSO lacks a significant UV absorption, the buildup of MTO was recorded. Both MTO and Me_2S were shown to be the products by their ^{1}H NMR spectra. For kinetics, these concentrations were used: 0.1 mM MDO, 16−700 mM DMSO; and both optical determinations and ^{1}H measurements (with ~1−5 mM MTO) are in agreement. These data and others are summarized in Table 3. Many of the listed substrates were studied by competition experiments, as presented in the Experimental Section. They relied on the thoroughly-studied DMSO as the reference compound.

Discussion

The H_3PO_2 Reaction. Tautomerization of $H_2P(O)OH$ to $HP(OH)_2$ is the initial step in several oxidation reactions, as with Br_2, I_2, and H_2O_2, for example.[40] The rate of the H_3PO_2−

---

(44) Espenson, J. H. *Chemical Kinetics and Reaction Mechanisms*, 2nd ed.; McGraw-Hill, Inc.: New York, 1995.

(45) Newton, T. W.; Baker, F. B. *Inorg. Chem.* **1964**, *3*, 569.

(46) Richens, D. T.; Sykes, A. G. *Comments Inorg. Chem.* **1983**, *1*, 141.

(47) Sasaki, Y.; Sykes, A. G. *J. Chem. Soc., Chem. Commun.* **1973**, 767.

Table 3. Rate Constants for Organic Oxo Compounds That React with Methylrhenium Dioxide (MDO)

substrate, XO	σ_p	$[XO]_0$/ mM[a]	k/L mol^{-1} s^{-1}	solvent, pH[b]	method[c]
Me_2SO		16−700	15.2 ± 0.1	100, 0	α
PhS(O)Me		1−3	17 ± 1	50, 0	β
PhS(O)Me		100, 200	17 ± 1	50, 1.24	χ
$MeC_6H_4S(O)Me$		100	21	50, 1.24	χ
$PhS(O)CH{=}CH_2$		100	11	50, 1.24	χ
Ph_3AsO		50	40	50 or 25, 1.24	χ
Ph_3SbO		20	55	50, 0 or 1.24	χ
$4\text{-}MeOC_5H_4NO$	−0.27	50, 100	7.80×10^3	100, 1.24	χ
$4\text{-}MeC_5H_4NO$	−0.17	50, 100	7.10×10^3	100, 1.24	χ
C_5H_5NO	0.00	100−200	4.60×10^3	100, 1.24	χ
$4\text{-}ClC_5H_4NO$	+0.23	150	2.67×10^3	100, 1.24	χ
$4\text{-}NCC_5H_4NO$	+0.66	200	6.5×10^2	100, 1.24	χ

[a] XO taken in large excess; $[MDO]_0$ was typically 0.05−0.2 mM. [b] Water vol % in CH_3CN-H_2O. [c] Methods: α = MTO buildup at 270 nm; β = sulfide buildup at 250 nm; χ = with NMR and chemical competition as in eq 4.

MTO reaction is higher than that of the tautomerization, however, eliminating that possibility.

Since this reaction displays an inverse kie, $k_H/k_D = 0.72$, rate-controlling hydride abstraction cannot be a valid mechanism. Instead, the kie reflects a P−H bond being weaker than an O−H bond, allowing us to speculate that O−H bond making is coincident with P−H bond breaking. An interpretation of the mechanism is found by invoking an intermediate analogous to those inferred during the exchange of oxygen atoms between MTO and water,[20,48] the initial step in the binding of hydrogen peroxide,[35] and the dehydration of alcohols,[49] as depicted here.

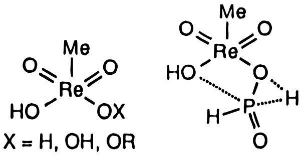

Next to that is a diagram showing the bond-making and bond-breaking events without, however, implying a sequential or concerted process.

Mechanism of O-Atom Transfer to MDO. The saturation kinetics for several of the oxoanions give direct evidence of adduct formation on the path for oxo transfer. The formation of Lewis acid−base adducts between MTO and organic oxygen donors such as sulfoxides[3] lends credence to the notion that MDO forms such an adduct prior to oxygen transfer. Adduct formation has been detected for reactions of organic oxygen-donors to Mo(IV) and Re(V) complexes.[6,10] In this instance the evidence was based on kinetics, not on spectroscopy, signaling that the MDO intermediates are highly reactive in comparison with the others. These reactions can be carried out in a catalytic manner, as illustrated in Scheme 2.

Further insight into the nature of the structure at the transition state was obtained from structure-reactivity correlations.[50,51] The rate constants for the pyridine *N*-oxides are correlated with the substituent constants σ, Table 3. Figure S-2, Supporting Information, shows a plot of $\log(k_X/k_H)$ against σ_X, the slope of which gives the reaction constant: $\rho = -1.18$. The linear correlation shows that the mechanism is common to all; the negative sign of ρ agrees with the assigned mechanism in which the nucleophilic pyridine *N*-oxides attack the electropositive rhenium center. Similar but perhaps less pronounced trends were found for the sulfoxides, Table 3.

Scheme 2

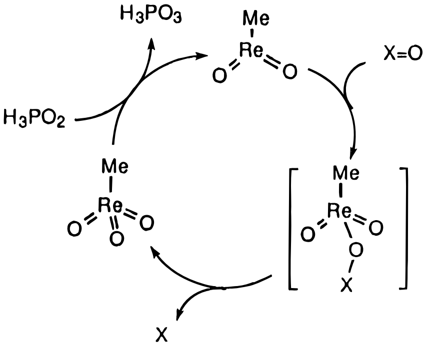

Reaction Thermodynamics. One can express gibbs free energy changes in one of three *equivalent* ways: from $E°$ data for the 2e half-reaction (eq 15a), for O-atom release (eq 15b), and for release of molecular oxygen (eq 15c). We illustrate these representations with the data for the perchlorate/chlorate and MTO/MDO reactions, the reference states being given explicitly:

		$\Delta G°$/kcal mol^{-1}		
reaction	symbol	ClO_4^-	MTO	
$XO(aq) + 2e^- + 2H^+ = X(aq) + H_2O$	$\Delta G_E°$	−55	−1	(15a)
$XO(aq) = X(aq) + O(g)$	$\Delta G_O°$	57	111	(15b)
$XO(aq) = X(aq) + {}^1/_2O_2(g)$	$\Delta G_{ox}°$	2	56	(15c)

The interconversion of the three Gibbs energy values is done with routine thermodynamic functions, and given any one of the values from the literature,[1,52,53] the others are immediately available. These equations are such relations:

$$\Delta G_O° = \Delta G_{ox}° + \Delta G_f°[O(g)]; \quad \Delta G_E° = \Delta G_{ox}° + \Delta G_f°[H_2O(l)] \quad (16)$$

We have chosen to show this detail to demonstrate the equivalency of these approaches. The literature may provide different parameters for different reactions, but all of the reactions can be put on the same scale, and any of the parameters cited carries exactly the same thermodynamic information content.

Since the reaction between V^{2+}, VO^{2+}, MTO, and MDO comes to a finite equilibrium, the value of its equilibrium constant allows the calculation of the same three values for MTO. They are shown in the list alongside the perchlorate ion entries. Over the pH range studied, necessarily narrow because of aforementioned limitations, the rate constant in each direction is independent of $[H^+]$.

Indeed, the vanadium−rhenium reaction provides a useful illustration. Whereas MDO reacts with DMSO and other O-atom donors fairly rapidly, V^{2+} is nonreactive with most of them, despite the fact that the thermodynamic driving force is the same. Likewise the reactions with perchlorate ion differ greatly as to rate: $k = 7.3$ L mol^{-1} s^{-1} for MDO and 2.2 ×

---

(48) Abu-Omar, M. M.; Hansen, P. J.; Espenson, J. H. *J. Am. Chem. Soc.* **1996**, *118*, 4966.

(49) Zhu, Z.; Espenson, J. H. *J. Org. Chem.* **1996**, *61*, 324.

(50) Hammett, L. P. *Chem. Rev.* **1935**, *17*, 125.

(51) Hammett, L. P. *Physical Organic Chemistry*; McGraw-Hill Book Co.: London, 1970.

(52) Latimer, W. M. *The Oxidation States of the Elements and their Potentials in Aqueous Solutions*, 2nd ed.; Prentice-Hall: New York, 1952.

(53) Bard, A. J.; Parsons, R.; Jordan, J. *Standard Potentials in Aqueous Solution*; M. Dekker: New York, 1985.

10^{-5} L mol^{-1} s^{-1} for V^{2+}.[54] The reactivity toward O-donors is not entirely thermodynamic in origin.

Nonetheless, it is instructive to explore a possible correlation between rate constants and driving force within the series of MDO reactions. The rate constants are given in Tables 2 and 3, and the values of $\Delta G°$ were obtained as the difference between MTO/MDO and the given substrate. Figure S-3, Supporting Information, illustrates the general failure of such correlations, even within homologous subseries of the whole. It seems to us the problems are these: (1) Driving force is but one of the involved parameters; in the sense of Marcus–Hush theory one needs to consider the intrinsic rates of O-atom exchange, such as the ClO_4^-–ClO_3^- interconversion; since they have not been determined we set this approach aside. (2) The thermodynamic data accurately reflect the overall reaction, but not necessarily the species to emerge from the transition state. Consider, for example, ClO_4^- vs VO^{2+}. The former, having transferred an O atom to MDO, emerges as ClO_3^-, at most with distorted angles and distances as compared to those of ordinary chlorate ion. On the other hand, O-atom abstraction from $(H_2O)_5VO^{2+}$ leaves immediately, one presumes, $(H_2O)_5V^{2+}$. Its Gibbs free energy differs from that of the hexaaquavanadium(II) ground state by a considerable but unknown amount.

In a general sense the high reactivity of MDO can be traced to the oxophilicity of high-valent rhenium, the considerable stability of MTO, and the relatively low coordination number of MDO.

We then made an attempt to correlate the rate constants with the force constants for the X=O bonds of the various substrates, determined from the frequencies for the asymmetric vibration. The first method, recorded in Figure 4, was simply to calculate a force constant from the vibrational frequency and the reduced masses by a diatomic approximation. This cannot be rigorously correct, of course,[55,56] but the results in a qualitative sense are nonetheless suggestive. The correlation is by no means exact, but certainly better than that provided by the thermodynamics of the overall reactions, no doubt because the force constant is a better measure of the activation barriers involved.

To pursue this, one really needs the force constant of an X=O bond obtained from a rigorous normal coordinate analysis.[55,56] This complex procedure has been carried out previously on a limited number of the substrates,[57–59] enough to attempt an analysis, as also shown in Figure 4. The force constants were obtained by applying the commonly used force field known as general valence force field (GVFF).[57] It seems that the compounds divide into natural classes by formula, within each of which there is a close conformity to the model, but not overall. We shall leave the matter at this point for now, having noted some possibilities for future development of the subject.

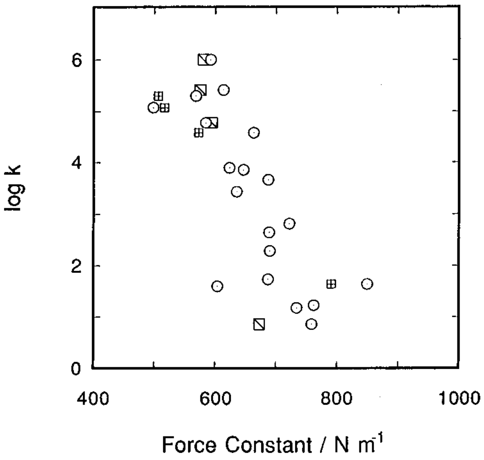

Figure 4. Log *k* for the reactions of MDO versus force constants for the asymmetric stretch of X=O bonds calculated from the vibrational frequencies and reduced masses assuming a diatomic model, shown as open circles. For a few of these species the force constant is known more exactly from a normal coordinate analysis applying GVFF, shown as partially-hatched and fully-hatched squares for XO_4^- and XO_3^-, respectively.

Acknowledgment. We are grateful to Ms. Jie Li for the determinations by ion chromatography. This research was supported by the U.S. National Science Foundation and by a U.S. Department of Education Fellowship awarded to M.M.A.-O.

Supporting Information Available: Time profiles for the reaction of MTO and H_3PO_2 at different concenentrations (illustrating the exceptional sensitivity of the oligomerization to concentration), the Hammett correlation for the reactions of pyridine *N*-oxides with MDO, and an attempted but unsuccessful LFER between log *k* and $\Delta G_{rxn}°$ for the reactions of MDO and XO (3 pages). Ordering information is given on any current masthead page.

IC960701Q

---

(54) King, W. R.; Garner, C. S. *J. Phys. Chem.* **1954**, *58*, 29.

(55) Nakamoto, K. *Infrared and Raman Spectra of Inorganic and Coordination Compounds*, 3rd ed.; John Wiley & Sons: New York, 1978.

(56) Drago, R. S. *Physical Methods for Chemists*, 2nd ed.; Saunders College Publishing: New York, 1992.

(57) Thirugnanasambandam, P.; Srinivasan, G. J. *J. Chem. Phys.* **1969**, *50*, 2467.

(58) Gardiner, D. J.; Girling, R. B.; Hester, R. E. *J. Mol. Struct.* **1972**, *13*, 105.

(59) Basile, L. J.; Ferraro, J. R.; Labonville, P.; Wall, M. C. *Coord. Chem. Rev.* **1973**, *11*, 21.